Energy Storage System by Means of Improved Thermal Performance of a 3 MW Grid Side Wind Power Converter

Qin, Zian; Liserre, Marco; Blaabjerg, Frede; Wang, Huai

Published in:
Proceedings of the 39th Annual Conference of the IEEE Industrial Electronics Society, IECON 2013

DOI (link to publication from Publisher):
10.1109/IECON.2013.6699226

Publication date:
2013

Document Version
Publisher's PDF, also known as Version of record

Energy Storage System by Means of Improved Thermal Performance of a 3 MW Grid Side Wind Power Converter

Qin, Zian; Liserre, Marco; Blaabjerg, Frede; Wang, Huai

Published in:
In Proc. of IEEE-IECON' 2013

DOI (link to publication from Publisher):
10.1109/IECON.2013.6699226

Publication date:
2013

Energy Storage System by Means of Improved Thermal Performance of a 3 MW Grid Side Wind Power Converter

Zian Qin, Marco Liserre, Frede Blaabjerg, Huai Wang
Center of Reliable Power Electronics (CORPE)
Department of Energy Technology, Aalborg University
Pontoppidanstraede 101, DK-9220 Aalborg East, Denmark
zqi@et.aau.dk, mli@et.aau.dk, fbl@et.aau.dk, hwa@et.aau.dk

***Abstract*—Wind speed variations make the power of wind turbine system to fluctuate, which could increase the thermal stress of the power converter and reduce its lifetime. In order to relieve this problem, short-term energy storage technologies are applied to improve the thermal performance of a 3 MW grid side wind power converter. The cost, weight and cycle life of the energy storage technologies are evaluated based on a typical low speed high turbulence wind profile. In detail, a wind turbine system model is established and its control strategy is illustrated, which is followed by the power control method of the energy storage system. Then the conventional thermal evaluation approach is simplified for evaluation with long term wind profile. The case studies are done to address the optimal power size and capacity of the energy storage system by comparing the improvement of the thermal performance. Also, the two promising candidates, ultracapacitors and batteries, are compared.**

Keywords—thermal performance; wind power converter; energy storage system; cost

I. INTRODUCTION

Wind Turbine System (WTS) technology is still booming among the renewable energy technologies [1-4]. The location is from onshore to offshore for smoother and more available wind source. The power rating of WTS is pushed to multi-MW to reduce the cost per kWh of the energy. As a consequence, the reliability of WTS is becoming more and more critical, because failure has large impact on the power generation and the maintenance of the high power offshore WTS is difficult and costs much. As reported in [5], one of the main areas of failure is the electrical system. Therefore, the reliability of wind power converters should be taken into account in order to ensure a high availability of the power source and also to obtain low maintenance cost.

According to the test data from the power semiconductor manufacturer and the Coffin-Manson model [6-8], the cycle life of power modules is dominated by their mean junction temperature together with the temperature cycling. Thus, the reliability of power converters can be improved by thermal-oriented control strategies as well as a good understanding of the mission profile combined with robust design. Several approaches have been proposed in order to achieve better thermal performance, in terms of optimizing of the modulation strategies, improving the topologies of the power converter, and reactive power control methods [9-11].

Energy storage technologies could solve the problems caused by the power fluctuations, a common barrier for most sustainable energy. Due to the scale of the capacity, energy storage technologies are usually classified into long-term and short-term [12]. Long-term ones, such as pumped hydro and compressed air, are usually used for power shifting, which means to move the additional electricity generation during the bottom of the consumption to the peak of the consumption. Short-term ones, such as batteries, ultracapacitors and flywheels, are mainly applied for power smoothing or frequency supporting of the power grid. In large scale WTS, the rotor with high moment inertia can be considered as a flywheel for energy storage, and it can be used for power smoothing [13], [14]. However, due to the limited energy storage capability of the rotor inertia, the power fluctuation in the wind power converter, which is smoothed by the rotor inertia, would still be able to induce significant thermal excursions of the power devices. An ultracapacitor is sized based upon the LVRT requirement for a DFIG wind turbine system, and it can also effectively damp short-term power oscillations and achieve superior transient performance. However, not much detail about the economical characteristics of the energy storage system is given; neither the reliability of wind power converters is taken into account [15].

In this paper, a short-term Energy Storage System (ESS) is applied in a multi-MW WTS to improve the thermal performance by power smoothing. Since the cost is the main barrier for application of ESS in high power and high capacity, the scope of this paper is to evaluate the power size, capacity at a fixed cost of the ESS, which is large enough for improvement of the thermal performance of wind power converters. In section II, a WTS model is established and its control strategy is illustrated. Then, in section III and IV the power control method of the ESS is proposed and the thermal evaluation approach is simplified for evaluation with long term wind profile. Finally, in section V case studies are done to address the optimal power size and capacity of the ESS by comparing the improvement on thermal performance. Moreover, the two promising candidates, ultracapacitors and batteries, are compared, where not only cost, but also weight and cycle life are taken into account.

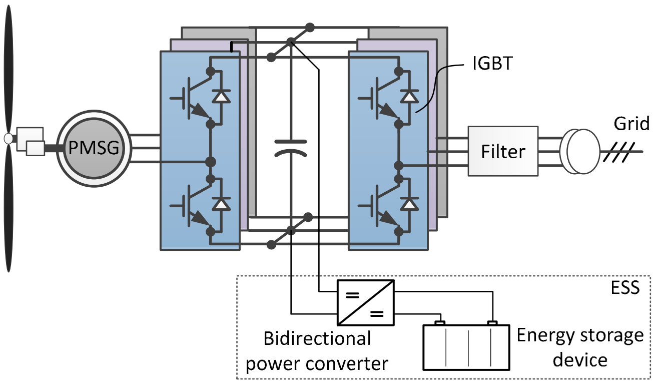

Fig. 1. Wind turbine system with full-scale power converter and energy storage system.

TABLE I.
WIND POWER SYSTEM PARAMETERS FOR 3 MW POWER LEVEL

Symbol	Name	Value
	Aerodynamic parameters	
R	Blade radius	46.9 m
$V_{w,in}$	Cut-in wind speed	3 m/s
$V_{w,r}$	Rated wind speed	12.5 m/s
$V_{w,off}$	Cut-off wind speed	25 m/s
$C_{p\,max}$	Maximum power coefficient	0.48
λ_{opt}	Optimal tip speed ratio	8.1
	PMSG parameters	
n_r	Rated rotor speed	15 rpm
N_g	Gear ratio	6.36
N_p	Number of pole pairs	20
ψ_m	Magnetic induced flux	2.8 Wb
L_s	Stator inductance	0.18 mH

II. WIND TURBINE SYSTEM

The structure of the wind turbine system is shown in Fig. 1. A single stage gearbox is applied to decrease the pole pairs of the Permanent Magnetic Synchronous Generator (PMSG) in order to avoid a large diameter. A conventional two-level back-to-back converter is employed for the power conversion from the generator to the grid. The aerodynamic and generator parameters are listed in Table I. The dc bus voltage is 1100 V which is a common choice for WTS considering that ac distribution line-to-line voltage is 690 V. The switching frequency is fixed at 2 kHz for both generator side and grid side converters.

The control structure for such a wind turbine system is shown in Fig. 2. For the generator side converter, an advanced torque mode control method [16] is applied to realize both maximum power point tracking (MPPT) and smoother power variations compared with speed mode control. Meanwhile, the current reference on d-axis $I^*_{s,d}$ is set to be zero to avoid damaging magnetic of the generator. For the grid side converter, the control strategy is to stabilize the DC bus voltage V_{dc} by regulating the active current $I_{g,d}$. The current on the q-axis can be controlled to regulate the reactive power injected to the grid. Since the power fluctuations are also related to the bandwidth of the controller, it should be noted that in MPPT, a first-order low pass filter with 5 s time constant is employed to deal with the measured wind speed in order to suppress the power fluctuations, and compared with it the dynamic performance of the other controllers is much faster. Therefore the impact of the control system on the power fluctuations is dominated by the low pass filter.

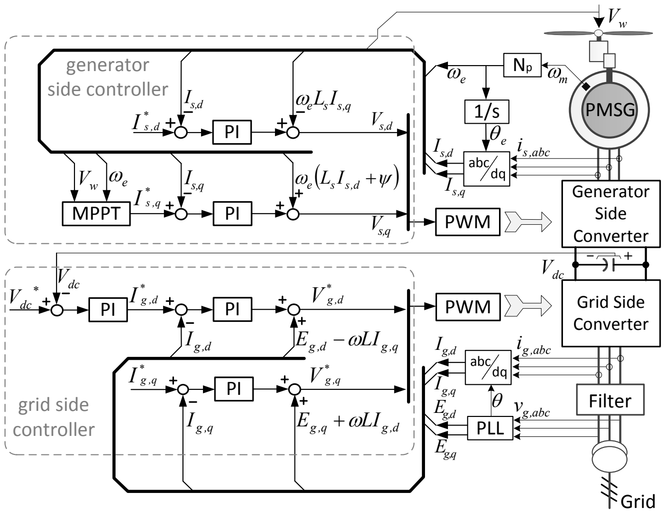

Fig. 2. Control scheme of wind turbine system without energy storage system.

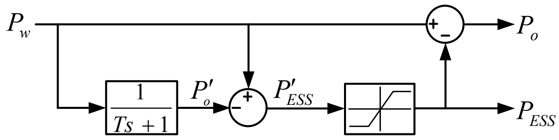

Fig. 3. Scheme of the power control for the energy storage system.

III. CONTROL STRATEGY OF ENERGY STORAGE SYSTEM

In order to reduce the thermal excursions of the grid side converter caused by the power variations, the ESS is connected to the DC bus, as seen in Fig. 1, and a low pass filter based power control strategy for the ESS is employed as illustrated in Fig. 3 [17]. The wind power P_w is filtered by a low pass filter with the time constant T in order to get smoother power flow P'_o, then the difference between P_w and P_o, marked as P'_{ESS}, is supposed to be the power injected into the ESS. However, considering the State Of Charge (SOC) and power rating of the ESS there should be a limitation for P'_{ESS}, as shown in Fig. 3. Then, the output of the limitation link, marked as P_{ESS}, is the power to be injected into ESS, and P_o, which is the difference between P_w and P_{ESS}, will be injected into grid through the grid side converter. It should be noted that the power fluctuation of the grid side converter would be influenced by not only the low pass filter but also the status of the ESS, in terms of SOC and power rating.

a. Design of the low pass filter

If the cutoff frequency of the low pass filter is defined as f_o, the following can be obtained,

$$f_0 = \frac{1}{2\pi T} \tag{1}$$

where T is the time constant of the low pass filter.

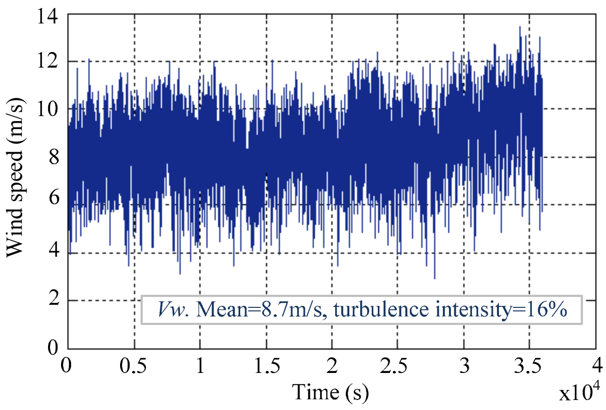

Fig. 4. A 10-hour long wind profile with low speed and high turbulence for evaluation.

The function of the low pass filter is to mitigate or reduce the short-term variation of the wind power, whose frequency f_s is typically 0.02~0.1 Hz [18], therefore the appropriate value for f_o is 0.002~0.01 Hz (f_o=f_s/10). According to (1), following can be obtained,

$$T=16\sim80 \text{ s} \tag{2}$$

Practically, the power rating of the ESS is not ideal, so in order to get more detail about its impact on the filtering performance of the ESS and also fix the value of time constant T, three study cases are done based on a typical low speed high turbulence (the ratio between the standard deviation and the mean value of the wind speed) wind profile, as seen in Fig. 4, and the time constant are set to be 5 s, 20 s, and 100 s, respectively.

The impact of the low pass filter on the power flow with various time constants in time domain is shown in Fig. 5. It can be seen that the output power of the filter (P'_o) becomes smoother with larger time constant; meanwhile the range of the input power of ESS (P'_{ESS}) becomes wider. Since the P'_{ESS} is relevant to the design of the power rating of the ESS, more comprehensive comparison is indicated by the distribution of P'_{ESS} in Fig. 6. As shown the distribution curve with larger time constant lies to the right side of the one with smaller time constant, which means the larger the time constant the higher the power of the ESS. Moreover, when T is 5 s, 0.14 MW power rating of ESS is needed in order to cover 50% of the requirement of the filter, the values of which are 0.21 MW and 0.29 MW respectively, for T=20 s and T=100 s. Due to the cost limitation of the ESS, the maximum power rating of the ESS is supposed to be 0.23 MW, which will be discussed in section V, thus the time constant will be set to 20 s.

The state of charge is another factor that may have impact on the performance of the ESS. Assuming there is no self-discharging in ESS and the charging/discharging efficiency equals to 100 %, the SOC can be obtained as follows,

$$SOC(t) = SOC(t_0) + \int_{t_0}^{t} P_{ESS}\, dt \tag{3}$$

where t_0 is the initial time. Since the wind power varies irregularly, it is quite probable that there is a dc bias in P_{ESS} with a longer period. In that case the ESS will be kept at high

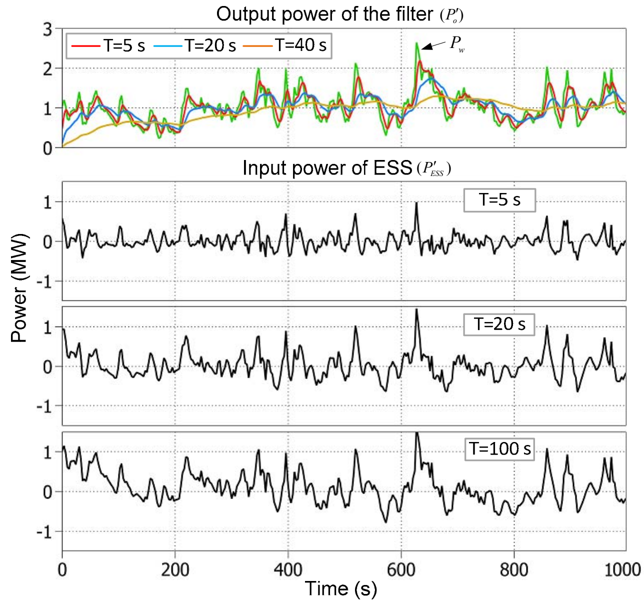

Fig. 5. The impact of the low pass filter on the power flow with various time constants in time domain.

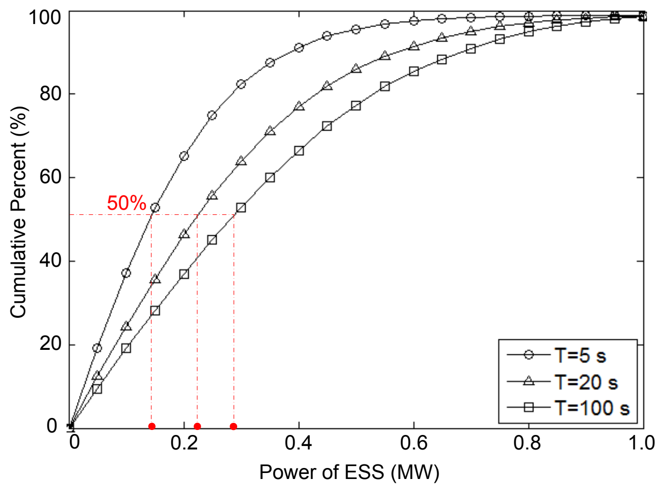

Fig. 6. The distribution of the power of ESS with various time constants.

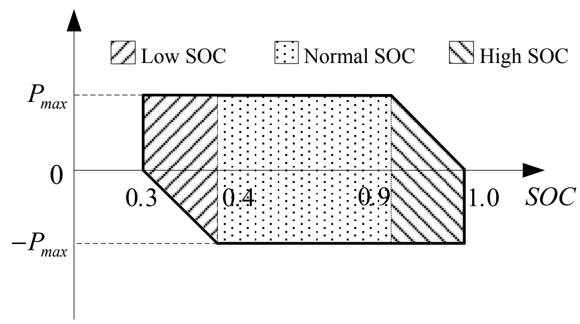

Fig. 7. Safe operation area of the energy storage system.

SOC or low SOC, which would reduce the utilization of the ESS, as shown in (3). In order to solve this problem, a variable power limitation method according to the SOC is proposed, as shown in Fig. 7. The safe operation area of the ESS is divided

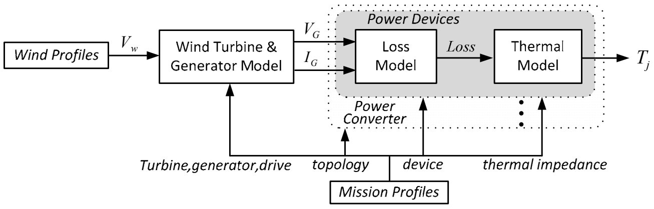

Fig. 8. Thermal performance evaluation method of wind power converter.

into three parts according to different SOC, low SOC (0.3-0.4), high SOC (0.9-1.0) and normal SOC (0.4-0.9). During normal SOC, the charging or discharging power P_{ESS} is limited by the power rating of ESS, which is $\pm P_{max}$. During low SOC, the discharging power is suppressed while the charging power limitation is still P_{max}. During high SOC, the charging power is suppressed, while the maximum discharging power is kept at P_{max}.

IV. THERMAL PERFORMANCE EVALUATION METHOD

The power size and capacity of the ESS are evaluated by measuring the improvement on thermal performance of the grid side power converter. The conventional thermal performance evaluation method is applied [19], as shown in Fig. 8. Firstly, the wind speed V_w is transferred to electrical power (V_G, I_G) by the wind turbine and generator model. Then with the loss model and thermal model the temperature of the power devices are gained.

The power loss is calculated based on a look-up table, where the switching loss is defined as a function of the blocking voltage and conduction current in order to reduce the computational effort [20]. The thermal model is composed of the power loss and thermal impedance between the different parts in the power devices. All of the data for the power loss model and thermal model of the power switch can be found in the product datasheet from the manufacturers. Actually, in this application, the HiPak IGBT Modules 5SNA 2400E170100 from ABB are employed. More details of the thermal model can be found in [11], [19].

It should be noted that the thermal behavior of the heatsink is more complicated for modeling, because it depends on the cooling technique, like air cooling and liquid cooling, and also the physical characteristic of the heatsink. In fact, the thermal capacitance of the heatsink is much larger than that of the power device, which means the temperature of the heatsink is much more stable than the power device. Therefore, the temperature of the heatsink is assumed to be constant at 50 ℃ for simplification.

Based on the above method, the thermal performance of the wind power converter with a specific wind speed can be investigated. However, in order to evaluate the thermal performance with a long wind profile, which is necessary for the evaluation of the power size and capacity of the ESS, the evaluation method needs to be simplified due to the simulation time. The power and junction temperature in the grid side converter based on a 10-min wind profile are evaluated with the thermal evaluation method mentioned above, and good correlation between the power and temperature profile is found, as seen in Fig. 9.

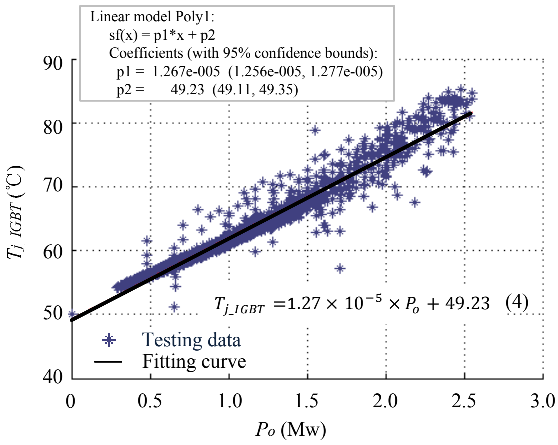

Fig. 9. Correlation between power and junction temperature in grid side converter.

It should be noted that, the good linear correlation between P_o and T_{j_IGBT} is more or less due to the assumption that the reactive power is zero and the heatsink's temperature is constant. But the assumption can be accepted in the evaluation of the ESS. According to (4), the loss model and thermal model in Fig. 8 used to obtain temperature from power can be simplified to shorten the simulation time. Meanwhile, the correlation between the wind speed and the power of the grid side converter is also investigated, but since the correlation is poor, the wind turbine and the generator model are still needed in the simplified thermal performance evaluation method.

V. EVALUATION OF ENERGY STORGAE SYSTEM

Since the proposed method is to utilize a small ESS with high power and low capacity to smooth the short-term wind power fluctuation, only two promising energy storage technologies Lithium-ion (Li-ion) batteries and ultracapacitors (Ultracap.) are considered. Due to the high complexity of the maintenance, the flywheel energy storage technology is not considered [21]. The physical and economical specifications of the two candidates are listed in Table II.

TABLE II. PARAMETERS OF THE ENERGY STORAGE TECHNOLOGIES [22-24].

	Ultracap.	Li-ion
Energy density (Wh/kg)	5	150
Power density (W/kg)	10000	1500
Costs for energy (€/Wh)	15	0.8
Costs for power (€/kW)	600	900
Cycle life	$>10^6$	$>10^3$

The total cost of ESS is calculated as the following [24],

$$Cost_{total} = UnitCost_E * E + UnitCost_{power} * P \quad (5)$$

where the $UnitCost_E$ is the unit capacity cost of the ESS and the $UnitCost_{power}$ is the unit power cost of the ESS, including the unit power cost of the energy storage device and the bidirectional power converter, which usually costs 700 €/kW. Assuming the cost of the ESS is fixed to be 1/10 of the total cost of the 3 MW WTS, which is typically 3 M€ [25], the function curve between the power and capacity of the ESS can be obtained based on (5) as shown in Fig. 10. The Li-ion

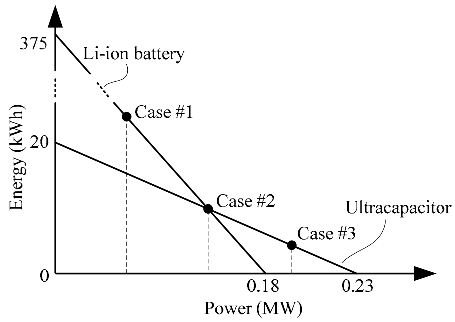

Fig. 10. Power and capacity of Li-ion battery and ultracapacitor with the same fixed cost.

TABLE III. SPECIFICATION OF THE ENERGY STORAGE CASES

	P (MW)	E (kWh)	Weight (t)	
			Ultracap.	Li-ion
Case #1	0.05	270	-	1.7
Case #2	0.177	6.25	1.25	0.12
Case #3	0.200	2.6	0.52	-

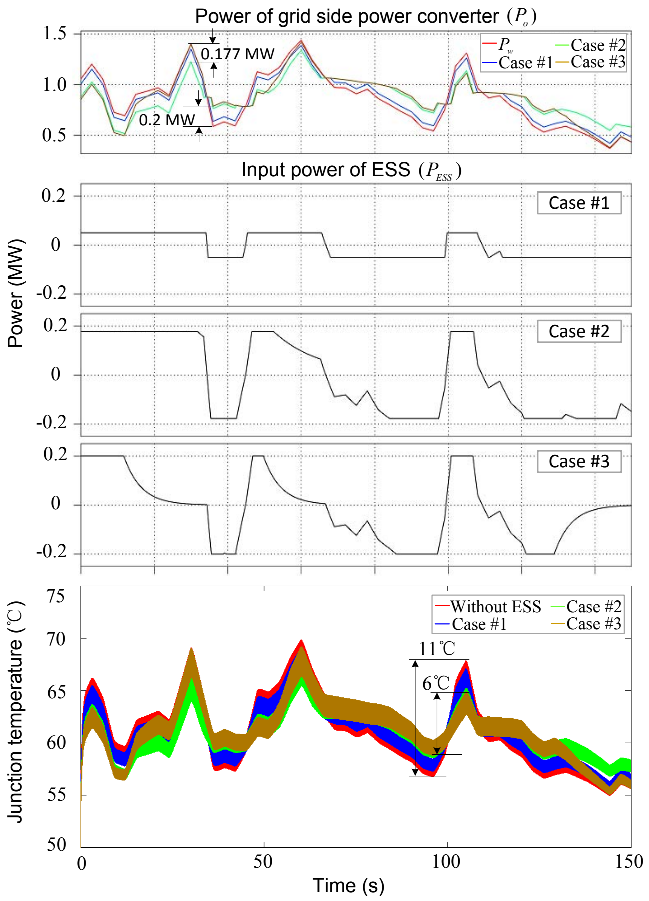

Fig. 11. Power behavior of the system and the thermal performance of the grid side power converter using energy storage.

battery has larger maximum capacity, which is 375 kWh, while the ultracapacitor has larger maximum power rating, which is 0.23 MW. In order to investigate the optimal power and capacity of the ESS and also the better choice between the two energy storage technologies, three cases with different power and capacity of the ESS are studied, as seen in Fig. 10. Case #2 is chosen to be the cross point of the two curves, where the two candidates have the same power and capacity. In case #1, the power of the two candidates is lower than case #2 and the Li-ion battery, which has higher capacity, is chosen. In case #3, the power is higher than case #2 and beyond the maximum power of the Li-ion battery, thus only ultracapacitor is chosen. The parameters of the three cases are listed in Table III.

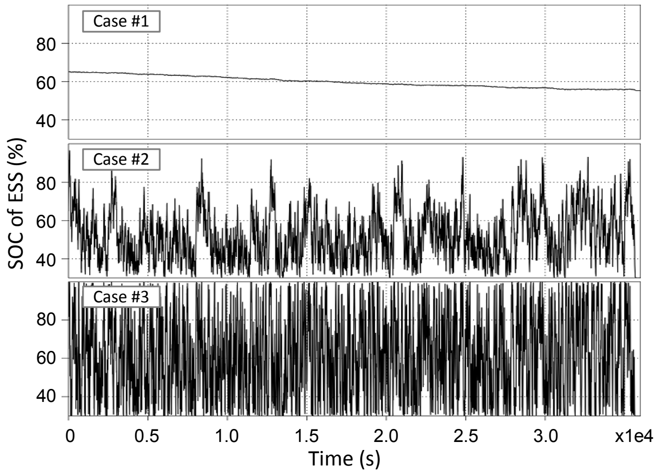

Fig. 12. State of charge for the energy storage system in time domain.

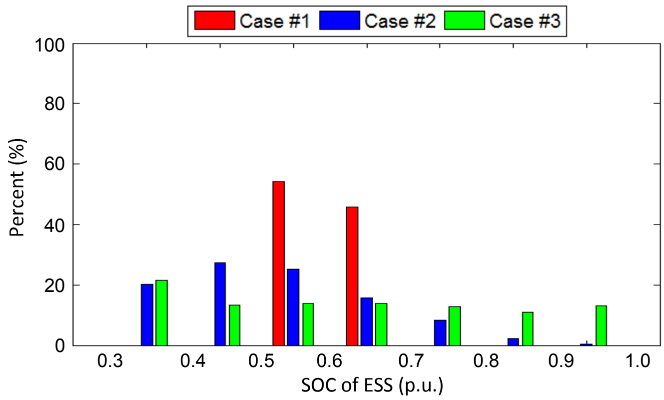

Fig. 13. Distribution of the state of charge for the energy storage system.

Power behavior of the system and the thermal performance of the grid side power converter are shown in Fig. 11. In case #1, as the power compensation capability of the ESS is low, the power of the grid side converter is almost the same with the case without ESS, thus little improvement on thermal excursions can be found. In case #2 and case #3, the power compensation capability of the ESS is relatively higher, therefore both the power and junction temperature of the grid side converter are smoother than in case #1.

In order to investigate the utilization of the energy storage of the ESS, the state of charge is compared both in time domain and by statistical approach, as shown in Fig. 12 and Fig. 13. Since the energy of the ESS decreases, its SOC becomes more unstable: the SOC in case #1 is kept in a quite narrow range, the SOC in case #3 is evenly distributed in the whole range, while the SOC in case #2 has a tradeoff performance between case #1 and case #3. It can be concluded that compared with case #2 and case #3, the energy utilization

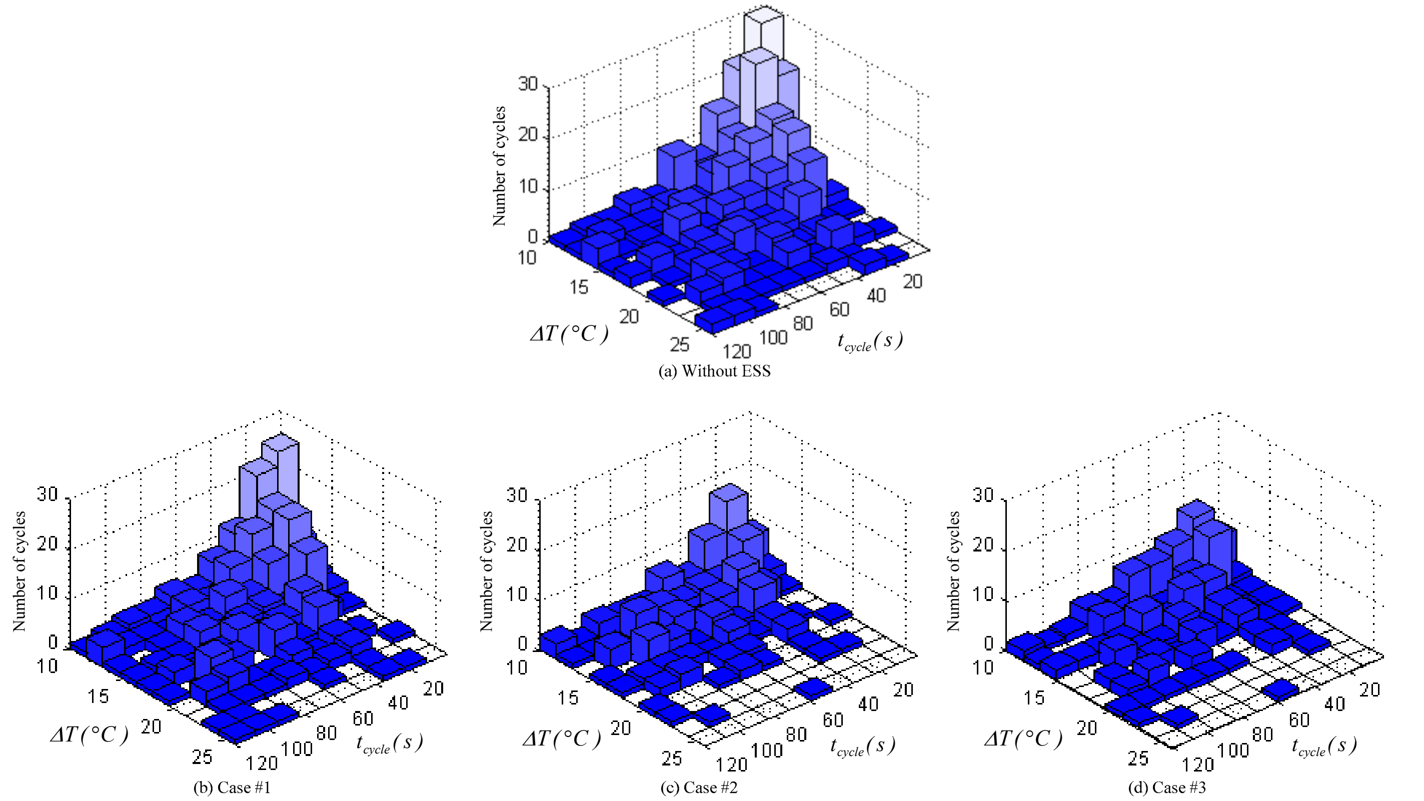

Fig. 14. Thermal performance of the grid side converter with or without energy storage system.

in case #1 is too low, which means the 270 kWh for the energy of ESS is far too large.

Based on the simplified thermal evaluation method mentioned above, the temperature of the power devices in different cases with the 10-hour wind profile is obtained. Then the thermal cycles are counted by Rainflow algorithm [26] and the distribution of the thermal cycles related to the amplitude (ΔT) and the period (t_{cycle}) can be seen in Fig. 14. Generally, compared with the thermal performance of the grid side converter in Fig. 15(a), where no ESS is employed, the thermal cycles are reduced to some degree when the ESS is applied. More details are,

- In case #1 (0.05 MW, 270 kWh), where the capacity of the ESS is much larger, the improvement on the distribution of the thermal cycles is not significant.
- In case #2 (0.177 MW, 6.25 kWh), where the power rating of the ESS is much larger than that of case #1, obvious improvement on distribution of thermal cycles can be found. Furthermore, the thermal cycles with amplitude ΔT above 20 ℃ are almost eliminated and the maximum number of thermal cycles is reduced from 30 to 18.
- In case #3 (0.2 MW, 2.6 kWh), where the power rating of the ESS is almost the same with case #2 and the capacity of the ESS is half, the improvement on distribution of the thermal cycles is almost the same with case #2.

It can be concluded that, high power of the ESS is more important than large capacity for improving the thermal performance of the grid side power converter. Moreover, in order to have the same improvement on thermal performance of the power converter, there is no large difference between Li-ion batteries and ultracapacitors from a cost perspective. But if the weight and cycle life are also taken into account, as shown in Table II and III, the ultracapacitors could be a better choice, because the weight of the ultracapacitor is not large and its cycle life is much longer than Li-ion battery. Another significant feature of the energy storage technologies is the charging/discharging time. For ultracapacitors, the value is 1 s, while for Li-ion batteries the value is 100 s [27]. Since the periods of most thermal cycles are between 1 s and 120 s, the ultracapacitors are better than Li-ion batteries from a dynamic point of view.

I. Conclusion

Energy storage technologies are sizing to reduce the power fluctuation in wind power converters and thereby to relieve the thermal stress. It can be concluded that a 200 kW and 2.6 kWh ultracapacitor module can be employed into a 3 MW wind power system for significant improvement on the thermal performance of the grid side converter, where the cost of the ESS is 1/10 of the total cost of the wind power system and the weight is 0.52 t, which is light enough to be put into the nacelle of the 3 MW wind power system. Additionally, the power of the ESS plays more significant role than capacity of the ESS for improving thermal performance of the grid side wind power converter. Therefore ultracapacitors, which also have much longer cycle life than Lithium-ion batteries, are better choice for this purpose. Although the cost of energy storage technologies in high power application is still high so far, there is an opportunity to utilize a small and relatively cheap ultracapacitor to obtain significant improvement of thermal performance of the grid side wind power converter, since the price of energy storage technologies keeps going down.

Reference

[1] F. Blaabjerg, Z. Chen, and S. B. Kjaer, "Power electronics as efficient interface in dispersed power generation systems," *IEEE Trans. Power Electron.,* vol. 19, no. 5, pp. 1184–1194, Sep. 2004.

[2] Z. Chen, J. M. Guerrero, and F. Blaabjerg, "A review of the state of the art of power electronics for wind turbines," *IEEE Trans. Power Electron.*, vol. 24, no. 8, pp. 1859–1875, Aug. 2009.

[3] M. Liserre, R. Cardenas, M. Molinas, and J. Rodriguez, "Overview of multi-MW wind turbines and wind parks," *IEEE Trans. Ind. Electron.*, vol. 58, no. 4, pp. 1081–1095, Apr. 2011.

[4] F. Blaabjerg, M. Liserre and K. Ma, "Power electronics converters for wind turbine systems" *IEEE Trans. on Ind. Appl.*, vol.48, no.2, pp.708-719, 2012.

[5] H. Berthold, M. Durstewitz and K. Rohrig, "Reliability of wind turbines," *Wind Energy*, Springer Berlin Heidelberg, 2007, pp. 329-332.

[6] ABB Application Note, *Load-cycling capability of HiPak^{TM} IGBT modules*, 2012.

[7] A. Wintrich, U. Nicolai and T. Reimann, "Semikron application manual," pp. 128, 2011.

[8] C. Busca, R. Teodorescu, F. Blaabjerg, S. Munk-Nielsen, L. Helle, T. Abeyasekera and P. Rodriguez, "An overview of the reliability prediction related aspects of high power IGBTs in wind power applications," *Microelectronics reliability*, vol. 51, no. 9-11, pp. 1903-1907, 2011.

[9] A. Isidori, F. M. Rossi and F. Blaabjerg, "Thermal loading and reliability of 10 MW multilevel wind power converter at different wind roughness classes," in *Proc. of ECCE' 2012*, pp. 2172-2179, 2012.

[10] F. Blaabjerg, K. Ma and D. Zhou, "Power electronics and reliability in renewable energy systems," in *Proc. of ISIE' 2012*, pp.19-30, 2012.

[11] K. Ma, M. Liserre and F. Blaabjerg, "Reactive power influence on the thermal cycling of multi-MW wind power inverter," *IEEE Trans. on Ind. Appl.*, vol.49, no.2, pp.922-930, 2013.

[12] M. Swierczynski, R. Teodorescu, C. Rasmussen, P. Rodriguez and H. Vikelgaard, "Overview of the energy storage systems for wind power integration enhacement," in *Proc. of ISIE' 2010*, pp. 3749 – 3756, 2010.

[13] L. Ran, J. R. Bumby and P. J. Tavner, "Use of turbine inertia for power smoothing of wind turbines with a DFIG," in *Proc. 11st IEEE International Conference on power quality 2004*, pp. 106-111, 2004

[14] A. Abedini, G. Mandic and A. Nasiri, "Wind power smoothing using rotor inertia aimed at reducing grid susceptibility," in *Proc. of IECON' 2008*, pp.1445-1451, 2008.

[15] C. Abbey, G. Joos, "Supercapacitor Energy Storage for Wind Energy Applications," IEEE Trans. on Ind. Appl., vol.43, no.3, pp.769-776, 2007.

[16] C. W. Lim, "Torque control methods for wind turbines and their responses," in *Proc. ICCAS' 2012*, pp.1788-1790, 2012.

[17] K. Yoshimoto, T. Nanahara and G. Koshimizu, "New control method for regulating state-of- charge of a battery in hybrid wind power/battery energy storage system," *in Proc. of PSCE' 2006*, pp.1244-1251, 2006.

[18] I. V. Hoven. "Power spectrum of horizontal wind speed in the frequency range from 0.0007 to 900 cycles per hour," *Journal of Meteorology*, 1957.

[19] ABB Application Note, Thermal Design of IGBT Modules, 2011.

[20] F. Blaabjerg, U. Jaeger and S. Munk-Nielsen, "Power losses in PWM-VSI inverter using NPT or PT IGBT devices," *IEEE Trans. Power Electron*., vol.10, no.3, pp. 358-367, May 1995.

[21] S. McCluer, J. Christin, "Comparing data center batteries, flywheels, and ultracapacitors," *White Paper 65*, Revision 2.

[22] D. I. Stroe, A. I. Stan, R. Diosi, et. al. "Short term energy storage for grid support in wind power applications," in *Proc. of OPTIM' 2012*, pp.1012-1021, 2012.

[23] Online available: http://batteryuniversity.com/learn/article/whats_the_role_of_the_ultracapacitor

[24] S. M. Schoenung, "Energy storage systems cost update," Sandia National Laboratories, Albuquerque, 2011.

[25] M. Bolinger, R. Wiser, "Understanding trends in wind turbine prices over the past decade," Lawrence Berkeley National Laboratory, 2011.

[26] ASTM International, *E1049-85 (2005) Standard practices for cycle counting in fatigue analysis*, 2005.

[27] J. R. Miller, "Operation and exploitation of electrochemical capacitor technology," in *seminar 18 of APEC' 2013*, 2013.